NASA Technical Memorandum 89860
AIAA-87-0994

Resistojet Control and Power for High Frequency ac Buses

Robert P. Gruber
Lewis Research Center
Cleveland, Ohio

NASA

RESISTOJET CONTROL AND POWER FOR HIGH FREQUENCY ac BUSES

Robert P. Gruber
National Aeronautics and Space Administration
Lewis Research Center
Cleveland, Ohio 44135

SUMMARY

Resistojets are operational on many geosynchronous communication satellites which all use dc power buses. Multipropellant resistojets were selected for the Initial Operating Capability (IOC) Space Station which will supply 208 V, 20 kHz power. This paper discusses resistojet heater temperature controllers and passive power regulation methods for ac power systems. A simple passive power regulation method suitable for use with regulated sinusoidal or square wave power was designed and tested using the Space Station multipropellant resistojet. The breadboard delivered 20 kHz power to the resistojet heater. Cold start surge current limiting, a power efficiency of 95 percent, and power regulation of better than 2 percent were demonstrated with a two component, 500 W breadboard power controller having a mass of 0.6 Kg.

INTRODUCTION

Resistojets are conceptually simple. The propellant is heated by convection, conduction, and/or radiation from a resistively heated element and then expanded through a nozzle to produce thrust. Resistojets were flight tested as early as 1965 (ref. 1).

NASA and others are developing multipropellant resistojet technology for the initial operating capability (IOC) Space Station and high performance resistojet concepts for spacecraft applications (refs. 2 to 12). Figure 1 is a photograph of the multipropellant resistojet engineering model and figure 2 is a cross-sectional sketch of this resistojet with the major features identified. The design choices, features, and construction details are reported elsewhere (ref. 3). The multipropellant resistojet must be integrated with the Space Station power system (ref. 13) which will be a 20 kHz, 208 V, single phase sinusoidal voltage bus.

The purpose of this paper is to present power bus integration considerations, design approaches, and performance characteristics for simple, passive, high efficiency, and lightweight power regulators for multipropellant resistojets operating from regulated ac power buses.

Basic design equations were derived describing power circuits which passively control resistojet heater power under conditions of varying heater resistance. Several candidate circuits were examined, some of which were suitable not only for regulated sinusoidal voltage buses, but regulated square wave voltage as well. A simple passive heater controller and cold start surge current limiter breadboard was built and tested with the engineering model resistojet. Tests results are compared with the design equations.

NOMENCLATURE

a   dimensionless variable

a_0 value of dimensionless variable that maximizes power, 3.212

A   leakage inductance referred to transformer secondary index for a given transformer core and winding geometry; $H/turn^2$

A_c effective cross-sectional area of a given transformer core, cm^2

B_{max} maximum flux density of transformer core, G

C   capacitance, F

f   frequency, Hz

i   instantaneous load current, A

I   load current, A rms

L   total inductance in secondary circuit, H

L_ℓ leakage inductance, H

n   secondary to primary transformer turns ratio

N_s transformer secondary turns

p.f.   load power factor at the bus

P   load power, W

P_N normalized load power; load power divided by load power at R_0

R   load resistance, Ω

R_0 load resistance that maximizes load power unless maximum $= \infty$, then $R_0 = 1$, Ω

R_N normalized load resistance, R divided by R_0

t   time, sec

T   period, sec

v   instantaneous secondary open circuit voltage, V

V   load voltage, V rms

V_{in} input voltage from bus, V rms

V_{oc} open circuit transformer voltage, V rms

X_c capacitive reactance, Ω

X_L inductive reactance, Ω

Z impedance, Ω

REQUIREMENTS

Spacecraft Considerations

The Space Station power distribution is regulated 20 kHz ac. A preliminary description of the Space Station power bus is given in table I (ref. 14). At this writing, more detailed specifications are being developed. The Space Station voltage is sinusoidal and closely voltage regulated. A few spacecraft have used square wave power buses. For example, the Mars Viking Orbiter had a relatively low power (~350 W) bus that used voltage regulated 2.4 kHz square waves (ref. 15). With regulated ac voltage, either sine wave or squarewave, a new set of passive and active resistojet control techniques becomes attractive.

Since detailed power system specifications were not available at this writing, it is necessary to speculate about some of the technical issues that could impact other Space Station systems. The first major issue would be user power profile. The power for each resistojet is only 500 W compared to the spacecraft nominal system power of about 75 kW. Therefore, cold start surge current and initial low power factor may not be serious concerns. A method of power control that results in a train of power pulses, a few seconds in length (depending upon the heater time constant), to provide for an average power need of less than 500 W has been suggested (ref. 16). Thus the bus would be pulse loaded, but at low power. Since this has significant system advantages, the power bus may be able to accommodate this regulation technique.

Another issue that could impact the bus is surge current that can be caused by transformer core remnant magnetization. Under conditions when the initial applied voltage causes the core flux to increase in the same direction as that of the remnant magnetization, the core saturates. The resulting steep increase in magnetizing current causes a short duration (of order 10 μsec), high amplitude current surge resulting in temporary voltage distortion. This uncertain, high intensity short duration surge is markedly different from the cold start surge current due to low heater resistance.

At 20 kHz, magnetic field electromagnetic compatibility requirements may become significant. The system Requirements and Interface Definition Study (ref. 4) reports that a preliminary analysis was conducted to estimate the level of electro-magnetic interference (EMI) generated within the resistojet. A heater wire loop near the nozzle contains 25 mm (1 in.) of wire without current in an adjacent wire in the opposite direction. A worst case estimate of the magnetic induction was about 102 dB above 1 pT which exceeds the MIL-STD 461B specification. The effect of the resistojet thermal insulation and outer case, and the distance from the resistojets to sensitive equipment must be determined. The report also states that if the magnetic induction is found to exceed actual requirements for user experiments, possible solutions include the following: (1) shield the resistojets with iron, (2) shield the experiments, (3) use a dc power supply, (4) devise a heater coil with no uncompensated length. Another potential technique to reduce radiated EMI is to take advantage of the fact that the thruster heater terminating leads also enclose an area that radiates a magnetic field. If the leads could be arranged so that

3

they enclose an equal area and that the current flows in the opposite direction, then this would help reduce the magnetic field at distances much greater than thruster length. The power controller may require one or more iron foil or thin walled case shields to meet the finalized spacecraft electromagnetic compatibility specification.

Thruster System Considerations

Preliminary resistojet control and power requirements for Space Station auxiliary propulsion and waste fluid management were described in a system requirement and interface definition study (ref. 4) for the Space Station engineering model resistojet (ref. 3). Key resistojet system control requirements were to limit heater temperature to 1400 °C with most propellants to ensure long life; and to assure that heater temperatures are less than 500 °C when using methane so free carbon is not produced; and to accommodate variable composition gases. The referenced study compared four heater control methods which were: (1) constant power and fixed inlet pressure (outlet gas temperature will vary, with specific impulse degrading for off nominal gas composition); (2) constant inlet pressure and variable power (the heater can be maintained near 1400°C for maximum specific impulse); (3) constant inlet pressure and two power settings; (most gases could be used at the high power level, mixtures containing methane or cabin air are used with the lower power level) and (4) constant power and variable flow control (heater temperature can be maintained near 1400 °C for maximum specific impulse). The four control methods were compared and the results presented in table II.

The tentative selection of the control power method was based on the desire for simplicity while sufficiently heating the propellants to provide about twice the room temperature specific impulse and to avoid condensation. The method uses constant inlet pressure with two power settings. Since the efforts reported in this paper are concerned primarily with heater control, it is noted that three of the four control methods studied required maintaining constant heater power. The fourth method requires constant heater temperature control. Heater control techniques for power and temperature will be discussed in detail later in the paper. An additional power control function may be required. As a precaution, to account for the condition of propellant flow interruption, a means of sensing heater over temperature and reducing power may be necessary.

At the 20 kHz bus frequency, thruster system skin and proximity effects should be taken into consideration, if ac is used for heater power. Handbook (ref. 17) calculations for the resistojet cold heater resistance show an increase of resistance of about 0.1 percent, considering only skin effects for the 1.52 mm (0.060 in.) diameter platinum - 10 percent rhodium heater element. The proximity effect of opposite direction currents in the adjacent heater windings is more difficult to determine since the calculated skin depth is large, 1.55 mm (0.061 in.) compared to the heater wire diameter and the interaxial heater wire separation of 3.15 mm (0.125 in.). However, the increase in resistance due to proximity effect will be less than 15 percent according to handbook information (ref. 17).

High performance hydrazine resistojet thrusters (ref. 10) used in geosynchronous communication satellites have tungsten heaters that exhibit hot to cold resistance changes of more than 10:1. The hydrazine resistojet systems

incorporate cold start surge current limiting (refs. 10 and 11). The long
life, multipropellant resistojet, which uses a platinum-10 percent rhodium
heater exhibits a 25 °C to 1400 °C heater resistance change of about 3:1. It
has not yet been established whether the Space Station resistojet itself
requires cold start surge current limiting to ensure reliable operation. The
issues could be potential risk of excess mechanical fatigue and contact resist-
ance degradation due to the many on-off cycles expected over the life of the
resistojet. Surge current and power limiting both ease the impact of these
concerns and make the thruster system a more friendly bus user.

Since the heater operates at low maximum voltages (20 to 30 V), a device
(e.g., transformer or ac to dc regulator) must be used to match the heater to
the high voltage (208 V) bus.

DESIGN

Design Philosophy

The design objective was to demonstrate a control and power electronics
concept specifically for the Space Station resistojet used in conjunction with
the 20 kHz sinusoidal power bus. However, the results are applicable to power
buses other than Space Station. Therefore, the suitability of the control
scheme developed when used with a square wave bus voltage was also investigated
and discussed in appendix A.

Of paramount importance to Space Station propulsion systems are life, low
maintenance, and simplicity. The Space Station multipropellant resistojet was
designed for lifetimes in excess of 10 000 hr with less emphasis on high per-
formance. In concert with this philosophy, the resistojet power controller
concept should be simple and capable of long life. Furthermore, the design
approach should provide adequate thruster system performance, high power effi-
ciency, and light weight.

The first issue is whether to power the resistojet heater with ac or dc.
Using dc alleviates the question of thruster magnetic field radiation; the need
to incorporate coaxial or special high current, high frequency transmission
lines and connectors; and can result in uncomplicated resistance measurement
circuits. However, changing the available, regulated ac power into dc power
reduces power efficiency, requires semiconductors, and complicates the power
train circuitry. Since the power bus detailed specifications and sub system
constraints are not yet completed at this writing, and since the control scheme
for the resistojet has not yet been finalized, resistojet heater power was
chosen to be ac for purposes of concept demonstration.

The next major issue considered is the method of control. For the work
described here, heater control will be considered only for ac heater power.
Of the four control options discussed earlier (ref. 4), three rely on constant
power control while one maintains constant heater temperature using variable
power. One technique for maintaining constant heater temperature is to deter-
mine and control the average heater resistance by varying heater power. This
technique has been used as a maximum temperature limiter for high performance
hydrazine electrothermal thrusters (ref. 18). The circuit was needed to pre-
vent overtemperatures due to momentary propellant loss or low pressure near end
of life when propellant flow would be low. The thruster heater formed one leg

5

of a resistance bridge that was supplied power through a series pass transistor. A control circuit maintained constant resistance by varying the current through the series pass transistor to keep the bridge balanced. Another control method, developed in Germany, that senses thruster temperature directly and controls the thruster using a microprocessor, has been designed, built and tested (ref. 9).

The writer has developed and tested closed loop resistance controllers using power dissipative and nondissipative techniques. The controllers operated from dc power sources and measured resistance from heater voltage and current signals. Some of the circuits were used in thruster characterization tests (ref. 19). Measuring and accurately controlling resistance from ac heater signals is much more difficult than with dc heater signals. For ac, heater inductance as well as skin and proximity effects must be considered in the design. If dc analog control circuits are used, the ac signals must be converted accurately to dc. Once suitable resistance determining signals are available, ac closed loop control techniques can be implemented.

For ac constant heater temperature control systems, the series pass control element can be a high power efficiency direct current controlled reactor (ref. 20) or a variable leakage inductance transformer (VLT) (ref. 21) instead of a semiconductor. These magnetic components can be rugged and reliable; however, the VLT is a fairly complex magnetic component. Direct current controlled reactors and VLT's are nonlinear and will create nonsinusoidal currents. These devices must be designed so that harmonic currents drawn from the bus are within bus specifications.

The effort described in this paper will concentrate on constant power control instead of resistance control. Constant power control provides an opportunity to achieve simplicity and was the preliminary thruster system heater control method selected as well as being employed in three of the four control methods discussed earlier (ref. 4). In keeping with the desire for thruster system simplicity and high reliability, a passive regulation scheme was designed, built, and tested.

Design Approach

The resistojet heater power and control concept is simply a current limiting transformer. This current limiting technique has been used for lighting applications and filament heating. The equivalent circuit for the transformer used in this work reduces to a voltage source driving an inductor in series with the variable resistance thruster heater. This simple equivalent circuit can be used for this particular current limiting transformer since the secondary open circuit inductive reactance is large compared to transformer leakage inductive reactance referred to the secondary and thruster heater resistance is large compared to the transformer winding resistance. The fundamental equations governing this power regulating method are listed in appendix B.

Figure 3 shows the transformer output characteristic. The transformer can also supply almost constant power over a wide range of resistances as seen in figure 3 when a constant power hyperbola is superimposed on the transformer output characteristic. Figure 3 also shows how the cold start surge current is limited. This power regulation technique is shown in figure 4 together with normalized power variations for current or voltage regulation versus normalized

resistance. The graph shows that power regulation of 0 to 5 percent is possible for nearly a 2:1 change in resistance. The technique has the potential disadvantage of low power factor (0.7 at maximum power), but at high frequencies (20 kHz), a high degree of passive power factor correction can easily be provided for almost no penalty.

Simple passive power factor correction at the power bus can be achieved for steady-state operation by using a shunt capacitor as shown in figure 5(a). With respect to the bus voltage, the lagging current in the current limiting transformer is added to the leading current in the capacitor. The resultant bus current is corrected for the transformer load power factor at one value of heater resistance as defined in equation (B11). The total load power factor will be leading or lagging depending upon the heater resistance. Power factor will vary according to equation (B10). The corrected power factor is nearly 1.0 for the range of heater resistances necessary for steady-state operation.

The change in power due to bus voltage regulation tolerance can be approximated using the total differential of power.

$$\frac{dP}{P} = \left(\frac{\partial P}{\partial V_{in}}\right) dV_{in} + \left(\frac{\partial P}{\partial R}\right) dR \tag{1}$$

For the constant power scheme described by equation (B5) in appendix B,

$$\frac{dP}{P} = \frac{2 \, dV_{in}}{V_{in}} + \left(\frac{X_L^2 - R^2}{X_L^2 + R^2}\right)\frac{dR}{R} \tag{2}$$

For conditions of nearly constant power, heater operation is near the maximum power point where R nearly equals $|X_L|$, so the second term in equation (2) is nearly zero during steady-state heater operation. Therefore,

$$\frac{dP}{P} \approx \frac{2 \, dV_{in}}{V_{in}} \tag{3}$$

and the 2.5 percent bus voltage regulation results in a heater power variation of about 5 percent.

Figure 5 shows several variations in implementation of the basic power control scheme. Table III compares the major advantages and disadvantages of each method. Multiple power setpoints can be provided using transformer tap changes, figure 5(b) or duty ratio pulsing, figure 5(c). A separate inductor in the primary figure 5(d) could be used to reduce initial current surges if remnant magnetization of the transformer core causes an unacceptable short duration initial current surge. Other means to reduce or eliminate the potential current surge due to remnant magnetization should the bus requirements dictate, include designing for a lower maximum flux density (higher weight); not choosing a square hysteresis loop magnetic material; making circuit provisions to set the core at a known flux direction and value; or using cores with a small gap.

The passive method of using a series capacitor and thruster resistance matching transformer figure 5(e), would result in the same current limiting

7

characteristic as the series inductor for sinusoidal waveforms, capacitive reactance current limiting is similar to inductive reactance current limiting and fundamental circuit considerations show that maximum power transfer occurs when the load resistance is equal to $n^2|X_c|$.

However, the power factor would be leading and difficult to correct since a shunt inductor is needed. At least two components would be needed instead of just one, but the method will have slightly less weight and slightly higher efficiency. Furthermore, if two thrusters need to be fired simultaneously, (such as opposing thrust waste fluid disposal), then the scheme in figure 5(e) could be paralleled with the method shown in figure 5(a) to provide a scheme, figure 5(f), that will maintain bus load power factor at nearly 1.0 during start up as well as steady-state operation. The capacitive reactance method was not evaluated further as part of this reported work.

Design Details

The scheme shown in figure 5(a) was designed, built, and tested with a thruster. The basic transformer technology was developed under the NASA Lewis Research Center power magnetics program (refs. 22 and 23). The 25 KVA transformer developed under this program featured a simple, reliable, and effective thermal control system. Furthermore, the 20 kHz transformer was lightweight and efficient. The basic mechanical configuration lended itself well to breadboard construction because no unusual fabrication techniques were necessary. Also, as part of the power magnetics program, transformer mass equations were derived from fundamentals. The equations were used to graph normalized specific weight versus magnetic flux density, power, and frequency. The graph is useful for resistojet system transformer mass predictions.

The 25 KVA, 20 kHz transformer developed under the power magnetics program was designed for low leakage inductance. The transformer used for this work requires a much higher leakage inductance for constant power and load current limiting characteristics. Developing accurate analytical expressions for leakage inductance based on the core and winding geometry was not practical because, for this transformer, leakage inductance calculations must take into account varying winding geometries as well as magnetic flux paths with changing flux densities (ref. 24). Therefore, an approximate expression developed for leakage inductance that incorporates an empirically determined constant, A:

$$L_\ell \cong AN_s^2 \tag{4}$$

A 10 turn trial winding was used together with a shorted turn primary (copper foil). Using equation (4) measurements of L_ℓ provided values of A for a variety of magnetic cores and winding arrangements.

The transformer equation (ref. 25) provides another design equation:

$$N_s = \frac{nV_{in}}{4.44 \times 10^{-8} A_c B_{max} f} \tag{5}$$

For this transformer, equations (4) and (5) combine to constrain the number of turns according to:

8

$$N_s = 4.44 \times 10^{-8} \frac{fL_\ell B_{max}}{nV_{in}} \frac{A_c}{A} \qquad (6)$$

The resistance value for maximum heater power was chosen using figure 4 together with the expected steady-state thruster heater resistance variations for the range of propellants at the pressure used. Once the value of thruster resistance required for maximum power was determined, the bus voltage, and equations (B5), (B8), and (B9), were used to obtain values for the turns ratio, n and the total inductance, L.

The total inductance, L necessary was 6.0 μH. The leakage inductance required was reduced by the heater and heater connecting wire inductances which totaled 1.6 μH, so only 4.4 μH, was needed for the leakage inductance, L_ℓ. The transformer core was selected using trial designs together with a selection of conveniently available magnetic cores, so that the transformer flux density was not near the saturation flux density, which was about 7 kg. A_c and A were adjusted to achieve a convenient N_s for a wire size and magnetic core that resulted in modest power loss. An adequate value of leakage inductance was easy to achieve for the 20 kHz current limiting transformer. The final flux density and all the transformer parameters are listed in table II. The mechanical construction details are shown in figure 6. No attempt was made to minimize the transformer mass or optimize its efficiency.

If the highest power efficiency or lightest weight becomes necessary instead of minimum parts count, then a separate inductor or capacitor in series with the transformer primary as shown in figures 5(d) and (e) should be considered.

Power factor correction to 1.0 was arbitrarily chosen at the maximum power point. The required value of capacitance was calculated using equations (B11) and (B12). The actual capacitor used was a standard value 0.10±0.01 μF foil – polypropelene dielectric capacitor rated by the manufacturer at 400 Vrms, 7 Arms. The cylindrical capacitor measured 1.43 cm (0.562 in.) diameter by 3.49 cm (1.375 in.) long and had a mass of 15 g. Equivalent series resistance (ESR) was not specified or measured, but the capacitor remained cool to the touch during tests at 208 V, 20 kHz.

TESTS

Loadbank Tests

A resistive load was used to determine power efficiency, transformer temperature rise, and to verify power factor correction and the transformer load characteristic. The power controller was tested at 208 rms, 20 kHz input power using several 0.10 Ω "noninductive" resistors in series. The inductance of the resistor network approximated the thruster and thruster lead inductance (1.6 μH) only at a load value of 0.7 Ω. For lower resistance values, extra inductance was added to total ~1.6 μH. Higher values of resistance had inductance values above 1.6 μH, yet adequate for load characteristic verification. For future tests, it may be easier to use a carbon pile load to keep the lead geometry and, therefore, the inductance approximately constant. For all tests reported, except the temperature rise test, a small fan was used to cool the transformer.

9

Measurements were made using three RMS voltmeters with analog readouts which had full scale accuracies of ±1 percent. Input and output voltages were measured directly. Output current was measured using a current transformer. A phasemeter measured the phase lag between the output current and the output voltage (at the transformer terminals). Power quality was checked using an oscilloscope. The input voltage was smoothly varying and almost sinusoidal. Real input power was measured using the 20 kHz generator power meter which was checked at 400 W using a "noninductive" resistor. The phasemeter input was voltage limited to 20 V. Special voltage dividers necessary to measure the input voltage phase relationship to transformer currents were not available so power factor correction was verified using an oscilloscope.

At an input of 208 V, with a 0.7 Ω, 1.6 μH load the following measurements were made: real input power, 542 W, output voltage, 20.05 V; output current, 26.9 A; phase between the output current and voltage, 16°. The real power out, calculated from the voltage, current and phase measurements was approximately 518 W which implies a power efficiency of about 95 percent.

The center heat sink temperature just below the windings was measured with a thermocouple. Steady-state temperature rise was measured for natural convection, with the transformer supported on an insulated benchtop. The test data are summarized in table IV.

Thruster Tests

The power controller was tested with the multipropellant resistojet mounted in a vacuum facility. The same electrical instrumentation that was used for the loadbank tests was used for thruster tests. The test configuration is shown in figure 7. Electrical data were recorded manually as well as with a slow (180 mm/hr) chart recorder. The thruster was instrumented with several thermocouples for other tests (ref. 5), so temperatures were also recorded. Tests were run at constant inlet pressure with helium, carbon dioxide, and argon, to span a range of propellant heat capacities which resulted in a corresponding range of resistances. For each gas, the thruster was started at room temperature and run until steady state was reached. Propellant line pressure, for each propellant, increased about 4.8 N/cm^2 (7 psia) as the thruster heated. Transient thruster data for argon and helium propellants are presented in figures 8 and 9 respectively. Heater power, current, resistance and heater sheath temperature are plotted as functions of time. Using this startup technique operating power was achieved in about 7 min. The thruster reached 90 percent of maximum resistance and heater temperature in about 20 min.

The power controller load characteristic at the thruster heater was calculated using equations from appendix B which required values of the measured secondary leakage inductance, thruster and connecting wire inductance, and open circuit voltage. The calculation neglects transformer winding resistances including skin and proximity effects. The calculated load characteristics and a 500 W constant power curve are plotted in figure 10 together with thruster test data and loadbank data. Loadbank data verify the transformer functional characteristics. Thruster data for steady-state operations as well as startup demonstrate surge current limiting and constant power operation.

10

Initial measured output power varied from 425 to 446 W. Calculated initial power output was about 404 W. The initial power was calculated for room temperature measured dc resistance (0.345 Ω) at the transformer secondary terminals. Accurate initial measurements were difficult since the heater resistance was changing rapidly and the power source voltage was drifting after initial turn on. The heater sheath temperature was measured on the last heater coil at the nozzle end. Steady-state test data for all propellants tested are listed in table V. Steady-state data for argon and helium are also available from figures 8 and 9. Power regulation is about 2 percent over the resistance range of 0.7 to 0.9 Ω heater resistance. Measured heater sheath temperature was 650° for helium and 1020 °C for argon. Heater steady-state temperature versus power data agree closely with dc power and temperature data from other tests (ref. 5).

DESIGN CONSIDERATIONS FOR AN ENGINEERING MODEL CONTROLLER

Further development effort should await more detailed power bus specifications as well as thruster system requirements. Radiated magnetic field restrictions will impact the controller mechanical and thermal designs. If the restrictions are quite severe, the magnetic component designs could change. A current limiting transformer with its greater leakage flux than conventional transformers may have to be replaced with a low flux leakage conventional transformer and separate current limiting capacitor or inductor in the primary circuit.

Based on tests with the unoptimized power controller, it is judged that passive power control meeting typical spacecraft thermal, EMI, and vibration specifications can be accomplished at power efficiencies of at least 97 percent and packaged mass of less than 2 kg for each 500-W thruster. Power regulation tolerance will equal twice the bus voltage tolerance (the bus voltage tolerance is ±2.5 percent at this writing) plus 2 or 3 percent due to the passive power controller characteristics.

There may be a need for an excessive temperature indication should propellant flow be interrupted. A single overtemperature indication signal can be obtained, if necessary, by adding a signal level winding near the secondary or by simply measuring the secondary voltage (the thruster heater is isolated from spacecraft structure). Since the transformer characteristic is fixed, the voltage is a function of heater resistance which in turn is a function of average heater temperature. This overtemperature indication method assumes adequate input bus voltage regulation. Bus transients and drop-outs can be easily accommodated with signal level components.

CONCLUSIONS

A simple, passive resistojet power controller was designed and tested to Space Station power bus specifications. The power controller delivered 20 kHz power to the Space Station multipropellant resistojet heater using a 208 V, 20 kHz sinusoidal power source. The thruster was operated at constant inlet pressure and constant power using helium, carbon dioxide and argon. Steady state thruster heater resistance ranged from 0.7 to 0.9 Ω for the three propellants used. Cold start surge current limiting, a power efficiency of 95 percent, and power regulation of better than 2 percent were demonstrated

with a two component, 500-W breadboard power controller having a mass of
0.6 kg.

Based on the breadboard tests, it is judged that a passive engineering
model power controller meeting typical spacecraft thermal, EMI and vibration
specifications can be developed having power efficiencies in excess of
97 percent and a packaged mass of less than 2 kg. for each 500-W Thruster.

APPENDIX A - EQUATIONS FOR A SQUARE WAVE VOLTAGE SOURCE

The purpose of this appendix is to determine the operating characteristics of the power controller for the special case where thruster systems are powered from a square wave voltage source.

When a current limiting transformer is used to supply the thruster heater, the equivalent circuit of the thruster system reduces to a square wave voltage source (transformer secondary open circuit voltage in series with the variable heater resistance, the heater and power cable inductance, and the transformer leakage inductance referred to the secondary).

The differential equation for a voltage source in series with a resistor and inductor is:

$$v(t) = L \frac{di}{dt} + iR \tag{A1}$$

Solving the differential equation for steady-state operation with a square wave voltage source over the half cycle when the voltage is positive yields:

$$i(t) = \frac{V_{oc}}{R} \left[1 - \frac{2e^{-tR/L}}{(1 + e^{-a})} \right] \quad \text{for} \quad 0 < t < \frac{T}{2} \tag{A2}$$

where

$$a = \frac{R}{2fL} \tag{A3}$$

is used for convenience.

The average power is found from

$$P = \frac{2R}{T} \int_0^{T/2} i^2(t)dt \tag{A4}$$

This results in

$$P = \frac{V_{oc}^2 T}{2L} \left[\frac{1}{a} - \frac{2}{a^2} \left(\frac{1 - e^{-a}}{1 + e^{-a}} \right) \right] \tag{A5}$$

An expression for maximum power is found by setting the first derivative of power with respect to a equal to zero and obtaining the roots of

$$\frac{1}{a^2} \left[\frac{4}{a} \left(\frac{1 - e^{-a}}{1 + e^{-a}} \right) - \frac{4e^{-a}}{(1 + e^{-a})^2} - 1 \right] = 0 \tag{A6}$$

Since equation (A6) cannot be solved in closed form, an iterative solution such as the Newton Raphson Method (ref. 26) must be used to obtain the root

13

$$a_0 = 3.212 \tag{A6}$$

and from equation (A3)

$$R_0 = 2 \times 3.212 \, fL \tag{A8}$$

An expression for normalized power, as a function of normalized resistance was obtained by substituting

$$a = R_N a_0 \tag{A9}$$

Then

$$P_N = \frac{\left[\dfrac{1}{R_N a_0} - \left(\dfrac{2}{R_N^2 a_0^2} \right) \left(\dfrac{1 - e^{-R_N a_0}}{1 + e^{-R_N a_0}} \right) \right]}{\left[\dfrac{1}{a_0} - \dfrac{2}{a_0} \left(\dfrac{1 - e^{-a_0}}{1 + e^{-a_0}} \right) \right]} \tag{A10}$$

When graphed, equation (A10) shows that the curve for square wave normalized power follows the curve for normalized sinusoidal power in figure 4 within 2 percent. Furthermore the equations defining R_0 for square waves and R_0 for sinusoidal power differ only by a constant. The slight difference is that for square waves the constant is 3.212, while the constant for sine waves is π.

Of course simple shunt capacitance power factor correction cannot be used for square wave voltage power buses.

APPENDIX B - EQUATIONS FOR A SINUSOIDAL VOLTAGE SOURCE

The fundamental equations governing the power regulating method are listed in this appendix. The equations are basic and describe a sinusoidal voltage source driving a series inductance resistance load. They are:

$$V_{oc} = nV_{in} \tag{B1}$$

$$|I| = \frac{V_{oc}}{|Z|} \tag{B2}$$

$$V = V_{oc} \frac{R}{|Z|} \tag{B3}$$

where

$$|Z| = \sqrt{X_L^2 + R^2} \tag{B4}$$

from which

$$P = n^2 V_{in}^2 \frac{R}{\left(X_L^2 + R^2\right)} \tag{B5}$$

and

$$P_N = \frac{2R_N}{R_N^2 + 1} \tag{B6}$$

where

$$R_N = \frac{R}{R_0} \tag{B7}$$

and

$$R_0 = |X_L| \tag{B8}$$

$$|X_L| = 2\pi f L \tag{B9}$$

Adding a shunt capacitor across the reflected series resistance-inductance load at the power bus will modify the power factor according to:

$$\text{p.f.} = \frac{R}{\sqrt{\frac{\left(|X_L|^2 + R^2 - n^2 |X_c||X_L|\right)^2}{n^4 |X_c|^2} + R^2}} \tag{B10}$$

From equation (A10) the value of X_c that will correct the load power factor to 1 at a specific value of heater resistance is:

$$|X_c| = \frac{1}{n^2} \left(|X_L| + \frac{R^2}{|X_L|}\right) \tag{B11}$$

The capacitance value is obtained from:

$$|X_c| = \frac{1}{2\pi f L} \tag{B12}$$

15

REFERENCES

1. Mirtich, M.J., "Resistojet Propulsion for Large Spacecraft Systems," AIAA Paper 82-1948, Nov. 1982.

2. Jones, R.E., "High and Low-Thrust Propulsion Systems for the Space Station," AIAA 87-0398, Jan. 1987.

3. Pugmire, T.K., Cann, G.L., Heckert, B., and Sovey, J.S., "A 10,000 Hour Life Multipropellant Engine for Space Station Applications," AIAA Paper 86-1403, June 1986.

4. Heckert, B.J., "Space Station Resistojet System Requirements and Interface Definition Study," RI/RD87-109, Rockwell International Corp., Canoga Park, CA, Feb. 1987. (NASA CR-179581).

5. Morren, W.E., Haag, T.W. and Sovey, J.S., "Engineering Model Resistojet Characterization," AIAA Paper 87-2120, May 1987.

6. Stone, J.R., "NASA Electrothermal Auxiliary Propulsion Technology," AIAA Paper 86-1703, June 1986.

7. McKevitt, F.X., "Design and Development Approach for the Augmented Catalytic Thruster (ACT)," AIAA Paper 83-1255, June 1983.

8. Dressler, G.A., Morningstar, R.E., Sackheim, R.L., Fritz, D.E. and Kelso, R., "Flight Qualification of The Augmented Electrothermal Hydrazine Thruster," AIAA Paper 81-1410, July 1981.

9. Schmitz, H.D. and Steenborg, M., "Augmented Electrothermal Hydrazine Thruster Development," Journal of Spacecraft and Rockets, Vol. 20, No. 2, Mar.-Apr. 1983, pp. 178-181.

10. Feconda, R.T. and Weizman, J.I., "Satellite Reaction Control Subsystem with Augmented Catalytic Thrusters," AIAA Paper 84-1235, June 1984.

11. Bingley, J.D., "Cold Start Surge Current Limiting System for a Hydrazine Thruster Augmentation Heater," U. S. Patent 4,523,429, June 1985.

12. McKevitt, F.X. and Schwam, F.R., "Design, Performance, and Operational Scaling Criteria for Electrically Augmented Hydrazine Thrusters," AIAA Paper 84-1234, June 1984.

13. Thomas, R.L., "Power is the Keystone," Aerospace America, Vol. 24, No. 9, Sept. 1986, pp. 36-38,40.

14. Terdan, F.F., Private communication, NASA Lewis Research Center, Cleveland, OH, Aug. 1986.

15. Decker, K., Private Communication, TRW Inc., Redondo Beach, CA, Mar. 1987.

16. Korn, I.I., Private communication, Rocketdyne Division of Rockwell International, Canoga Park, CA, Aug. 1986.

17. Terman, F.E., <u>Radio Engineers' Handbook</u>, McGraw-Hill, New York, 1943.

18. Hosick, D. and Rentella, W., Private communication, Ford Aerospace, Nov. 1984.

19. Morren, W.E., Whalen, M. and Sovey, J.S., "Performance and Endurance Tests of a Multipropellant Resistojet for Space Station Auxiliary Propulsion," AIAA Paper 86-1435, June 1986.

20. Aggers, C.V. and Pakala, W.E., "Direct-Current Controlled Reactors," <u>Electric Journal</u>, Vol. 34, No. 2, Feb. 1937, pp. 55-59.

21. Hirayama, H., "Simplifying Switched Mode Converter Design with a New Variable Leakage Transformer Topology," <u>Proceedings of Powercon 7</u>, R.I. Birdsall, ed., Power Concepts Inc., Ventura, CA, 1980, pp. E1-1 to E1-10.

22. Schwarze, G.E., "Development of High Frequency Low Weight Power Magnetics for Aerospace Power Systems," <u>Advanced Energy Systems - Their Role In Our Future</u>, Vol. 1, American Nuclear Society, LaGrange Park, IL, 1984, pp. 196-204.

23. Welsh, J.P., "Design and Development of Multi-kw Power Electronic Transformers," TTL-83-1, Thermal Technology Labs, Buffalo, NY, Feb. 1983. (NASA CR-168082).

24. Slemon, G.R., <u>Magnetoelectric Devices</u>, John Wiley & Sons, New York, 1966.

25. <u>Magnetic Circuits and Transformers</u>, John Wiley & Sons, New York, 1943.

26. Scarborough, J.B., <u>Numerical Mathematical Analysis</u>, Johns Hopkins Press, Baltimore, 1955.

TABLE I. - PROVISIONAL SPACE STATION POWER BUS DESCRIPTION (ref. 14)

[August 1986.]

Item	Description	Comments
Nominal system power	75 kW	
Frequency	20 kHz ± 0.1 percent	Sinusiodal waveform
Voltage	208 V rms ± 2.5 percent	At user loads
Power factor	0.9 Minimum lagging	Specified for entire power system
Total harmonic distortion	3 percent	
Drop out duration	50 msec Maximum	
Transient voltage	±10 percent Maximum for 250 µsec	
Electromagnetic compatibility	Mil-STD-461B including RE-01 to be amended	Must be adequate for scientific payloads (plasma experiments)

TABLE II. – COMPARISON OF RESISTOJET CONTROL METHODS (ref. 4)

Methods	Advantages	Disadvantages
1. Constant power and fixed pressure	Simplest. Can be low power to be consistent with cabin air and methane require-ments	Specific impulse degradation
2. Constant pressure and variable power	Near optimum specific impulse for all gas compo-sitions	Most complicated power control
3. Constant pressure and two-power setting[a]	Higher specific impulse than method 1, Retains power control simplicity. Compatible with methane and air	Specific impulse degradation for some propellants
4. Constant power and variable flow control	Optimum specific impulse for all gas compositions	Flow control more complicated than constant pressure regulation

[a]Tentative selection.

TABLE III. - COMPARISON OF POWER REGULATING METHODS

Methods	Advantages	Disadvantages
Figure 3(a) Single power setting	Physically simplest - (one component) Power factor correction capacitor is optional	High power efficiency current limiting transformer design more difficult than standard transformer design Potential disadvantage of remnant magnetization Transformer steady-state VA rating is $\sqrt{2}$ times maximum heater power
Figure 3(b) Two power setting	Bus power not pulsed	Requires two power switches
Figure 3(c) Two or multiple power settings	Requires only one power switch	Bus power is pulsed. Pulsing control circuits are needed
Figure 3(d) Separate inductor in primary	Potential remnant magnetization problem is eased Transformer steady-state VA rating about equal to heater power Easier to design a high efficiency transformer	Extra power magnetic component with attendant power loss and weight
Figure 3(e) Series capacitor in transformer primary	Transformer steady-state VA rating about equal to heater power Can achieve highest efficiency and lightest weight	Leading power factor not easily corrected Requires at least two components, while figure 3(a) needs only one
Figure 3(f) Dual power regulator scheme	Maintains bus load power factor near 1.0 during turn on transient as well as steady state. Corrects power factor and regulates two thrusters with three components	Requires simultaneous operation of two thrusters

TABLE IV. - BREADBOARD TRANSFORMER DATA

Item	Description
Core	MC-1717-1D Magnetics Incorporated, core gap faces lapped and polished
Primary winding	66 Turns No. 18 AWG: 3 copper heat sink winding assemblies, each with two 11 turn, single layer, pancake windings cemented to each side of a 0.079 cm (0.031 in.) thick, copper plate insulated with a thin polyimide film.
Secondary winding	9 turns: 4 paralleled No. 16 AWG windings: 2 copper heat sink winding assemblies, each with two 9 turn windings constructed the same as the primary winding assemblies.
Primary dc resistance	0.156 Ω at 25 °C (measured)
Secondary dc resistance	0.0034 Ω at (25 °C) (measured)
Secondary open circuit inductance	510 μH (measured)
Leakage inductance referred to secondary	4.4 μH (measured) Adjustable from 3.3 to 8.6 μH by positioning primary and secondary winding locations. Centered windings produce 3.3 μH; primary, and secondary windings located at opposite ends result in 8.6 μH leakage inductance
Maximum flux density	2.75 kilogauss at 208 V input, 20 kHz
Core loss	6 W, (from manufacturer's data)
dc winding loss	5.9 W at 100 °C, 26.9 A secondary current
Measured total loss	approximately 24 W, 208 V input, 26.9 A output, 20 kHz with a 1.6 μH, 0.7 Ω dc load.
ac eddy current and skin effect losses	or order 12 W estimated from measured total loss minus calculated core and dc winding losses
Power efficiency	Approximately 95 percent (measured using power meter, 208 V input, 26.9 A output, 20 kHz with a 1.6 μH, 0.7 Ω dc load)
Temperature Rise	84 °C with natural convection at center of middle copper heat sink measured with 208 V in, 27.3 A out
Mass	0.590 kg including heat sink clamp

TABLE V. - RESISTOJET POWER CONTROLLER TEST DATA

Propellant	Propellant pressure, N/cm^2	Power, W	Heater resistance, Ω	Heater sheath temperature, °C	Calculated power controller bus power factor[a]
Steady-state data					
Argon	30.8 (44.7 psia)	485	0.91	1020	0.980 leading
Carbon Dioxide	30.8 (44.7 psia)	493	0.80	820	0.998 leading
Helium	29.0 (42.1 psia)	490	0.71	650	0.999 lagging
At startup					
All propellants	All pressures	404[b]	0.345[c]	25 °C	0.766 lagging

[a]Calculated for C = 0.10 μF, L = 6.0 μH.
[b]Calculated from measured dc resistance and L = 6.0 μH.
[c]dc measurements at transformer connection.
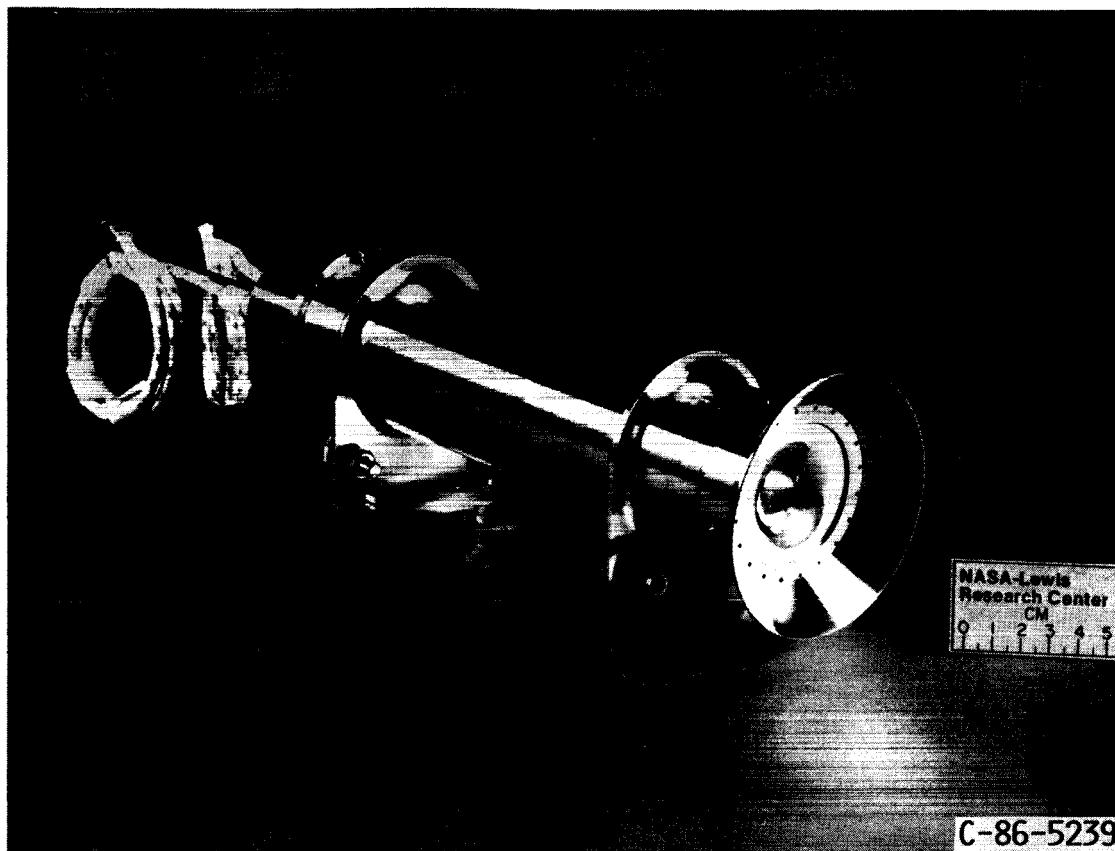
FIGURE 1. - ENGINEERING MODEL OF RESISTOJET.

PLATINUM SHEATHED HEATER
(PT CENTER CONDUCTOR, MgO
INSULATOR, PT SHEATH)

CONE/TRUMPET NOZZLE

(3.8 IN.) 9.65 CM

(0.040 IN.) 0.10 CM DIAMETER THROAT

PLUME SHIELD

NI RADIATION SHIELDS

PT RADIATION SHIELDS

(9.4 IN.) 23.9 CM

(0.4 IN.) 1.02 CM

MOUNTING BRACKET

OUTER CASE (INCONEL)

MULTI-CHANNEL HEAT EXCHANGER

PROPELLENT INLET

(2.4 IN.) DIAMETER 6.10 CM
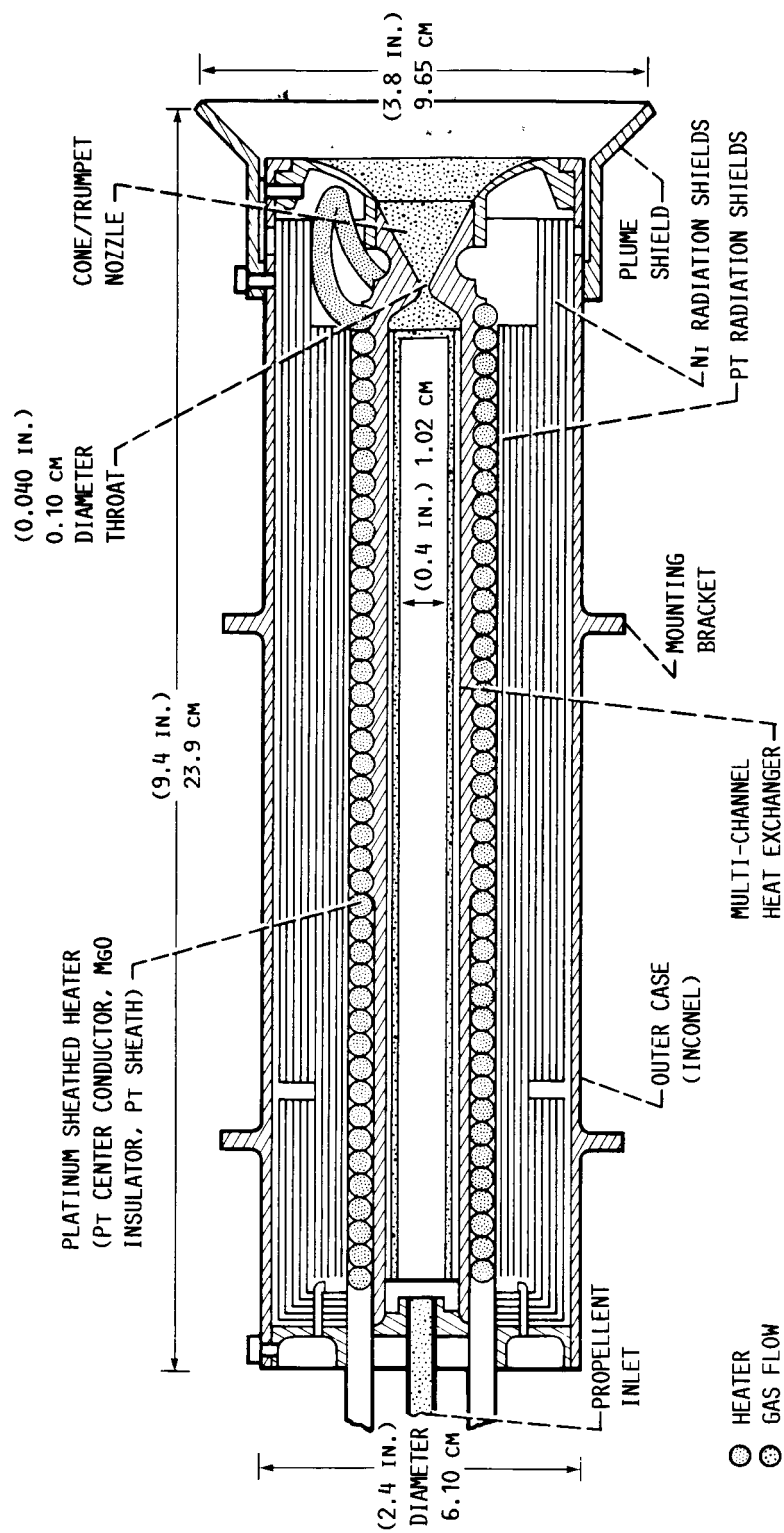
◎ HEATER
⊕ GAS FLOW

FIGURE 2. – CROSS-SECTIONAL SKETCH OF ENGINEERING MODEL OF RESISTOJET.
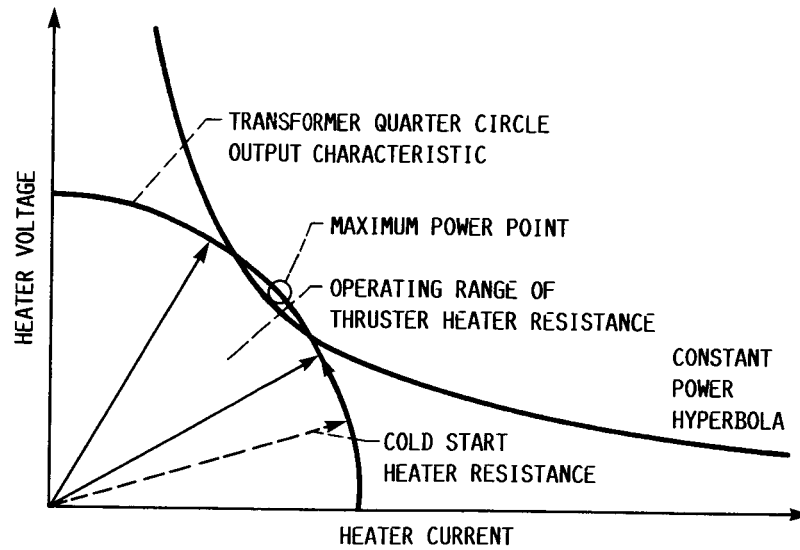
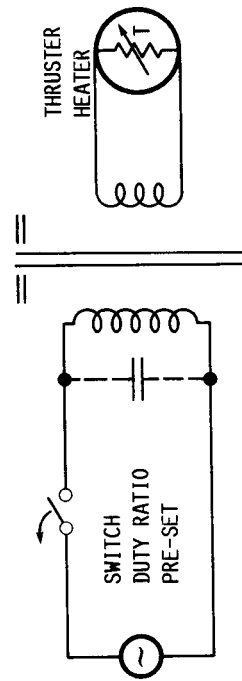FIGURE 3. - THRUSTER HEATER AND TRANSFORMER OUTPUT CHARACTER-
ISTICS.
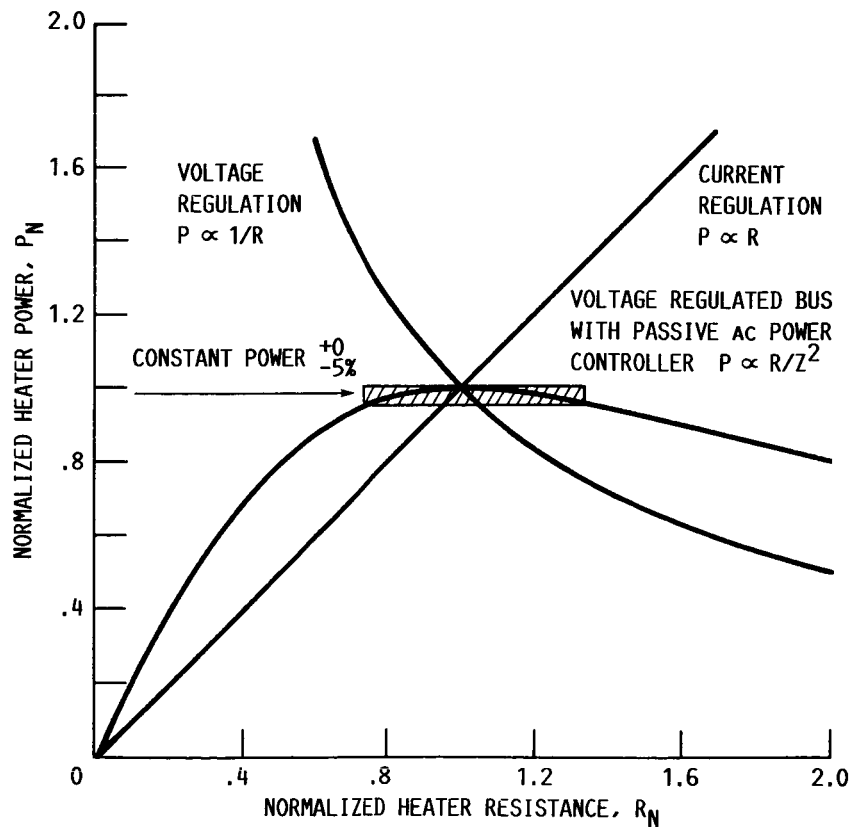
FIGURE 4. - RESISTOJET CALCULATED NORMALIZED POWER VERSUS
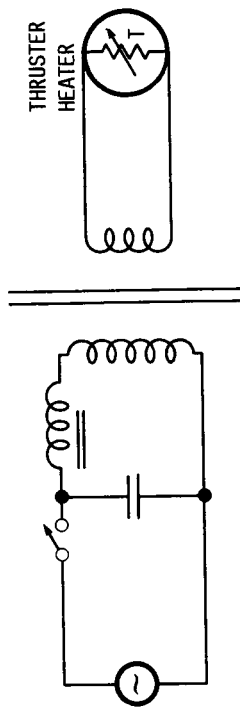NORMALIZED HEATER RESISTANCE.
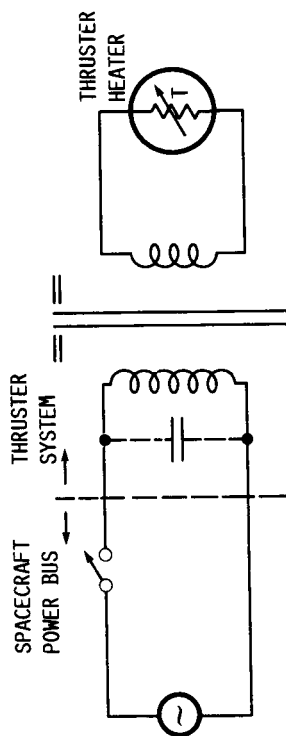
(A) SINGLE SETTING POWER REGULATOR AND COLD START SURGE CURRENT LIMITING METHOD (TESTED WITH THRUSTER).
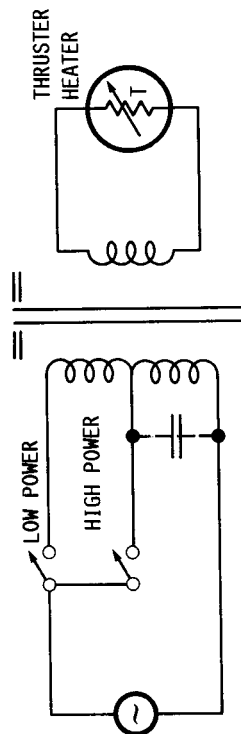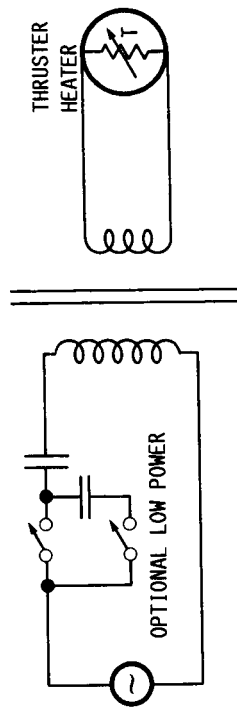
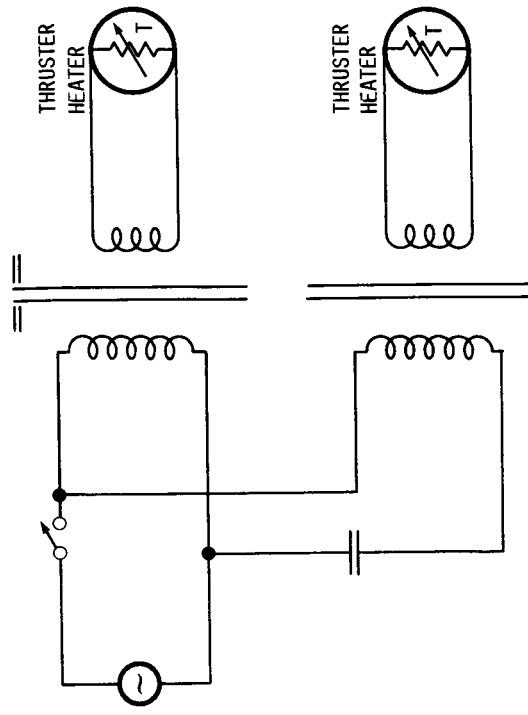(B) ALTERNATE DUAL POWER SETTING POWER REGULATOR.

(C) ALTERNATE DUAL OR MULTIPLE POWER SETTING POWER REGULATOR.

(D) POWER REGULATOR WITH SEPARATE INDUCTOR IN THE PRIMARY.

(E) POWER REGULATOR COLD START SURGE CURRENT LIMITING SCHEME USING SERIES CAPACITOR.

(F) DUAL POWER REGULATOR SCHEME TO MAINTAIN BUS LOAD POWER FACTOR NEARLY 1.0.

FIGURE 5. - PASSIVE RESISTOJET POWER REGULATION AND COLD START SURGE CURRENT LIMITING METHODS.
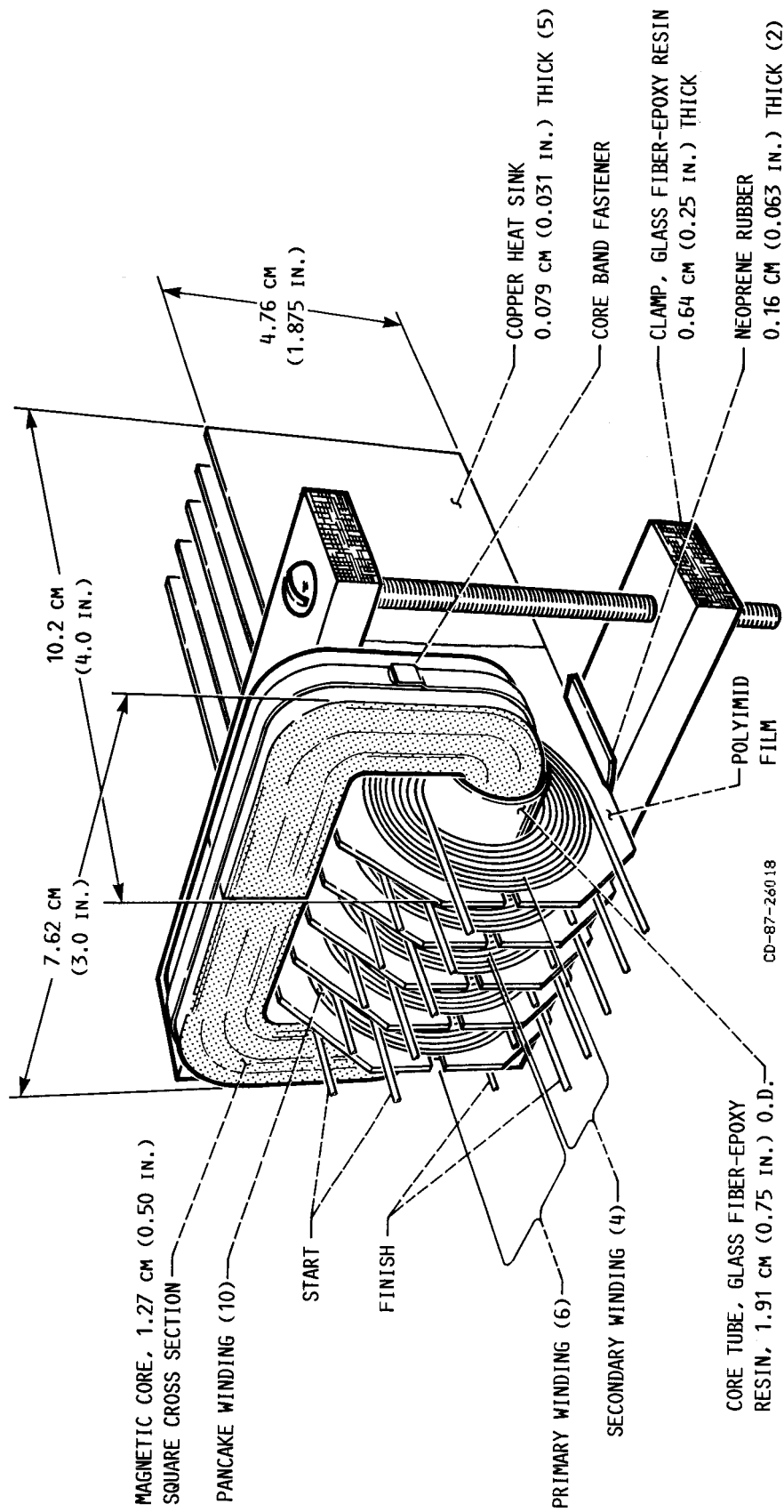
26

MAGNETIC CORE, 1.27 CM (0.50 IN.)
SQUARE CROSS SECTION

PANCAKE WINDING (10)

START

FINISH

PRIMARY WINDING (6)

SECONDARY WINDING (4)

CORE TUBE, GLASS FIBER-EPOXY
RESIN, 1.91 CM (0.75 IN.) O.D.

COPPER HEAT SINK
0.079 CM (0.031 IN.) THICK (5)

CORE BAND FASTENER

CLAMP, GLASS FIBER-EPOXY RESIN
0.64 CM (0.25 IN.) THICK

NEOPRENE RUBBER
0.16 CM (0.063 IN.) THICK (2)

POLYIMID
FILM

4.76 CM
(1.875 IN.)

10.2 CM
(4.0 IN.)

7.62 CM
(3.0 IN.)

CD-87-26018

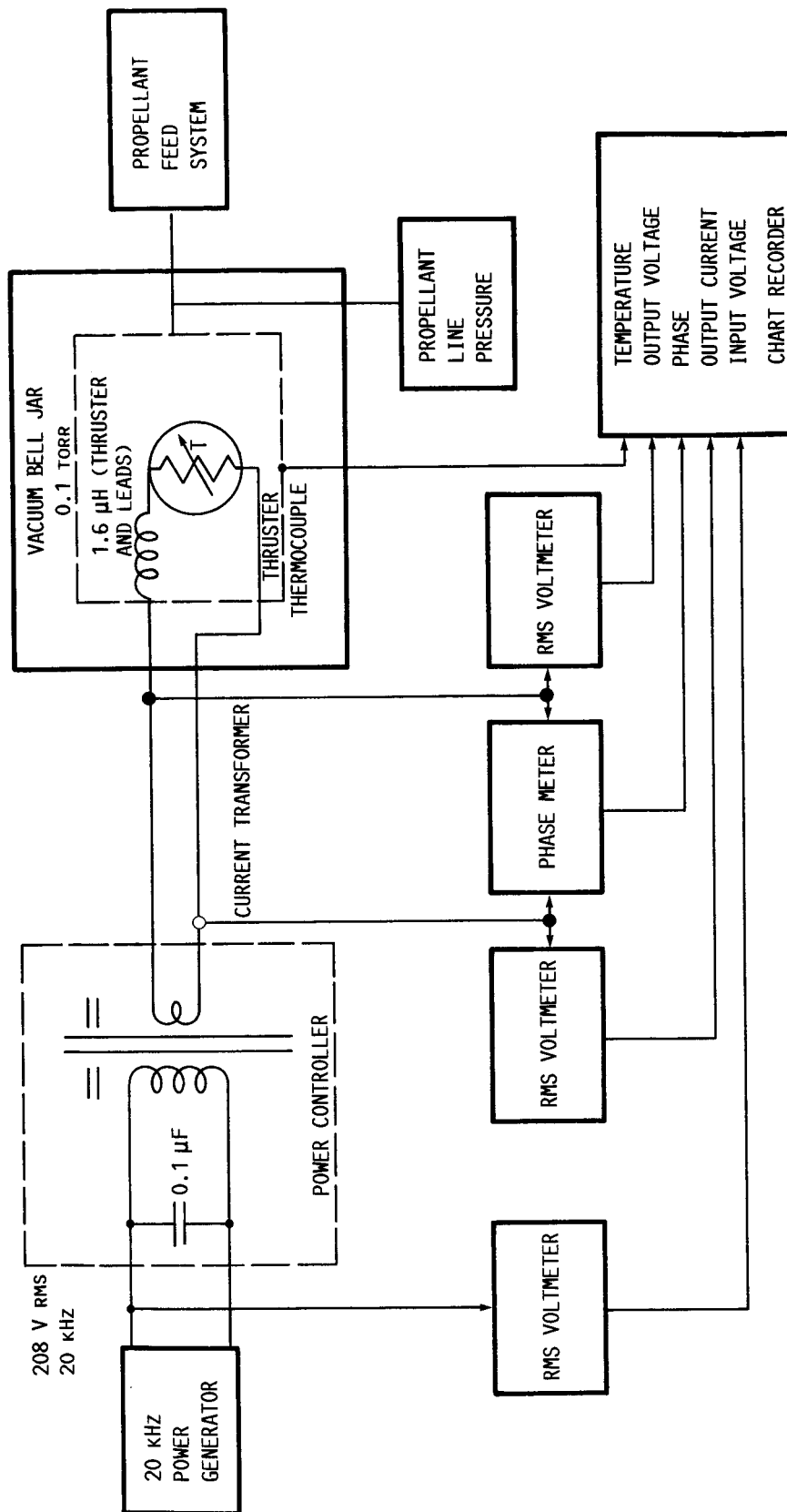FIGURE 6. - ILLUSTRATION OF BREADBOARD TRANSFORMER.

27

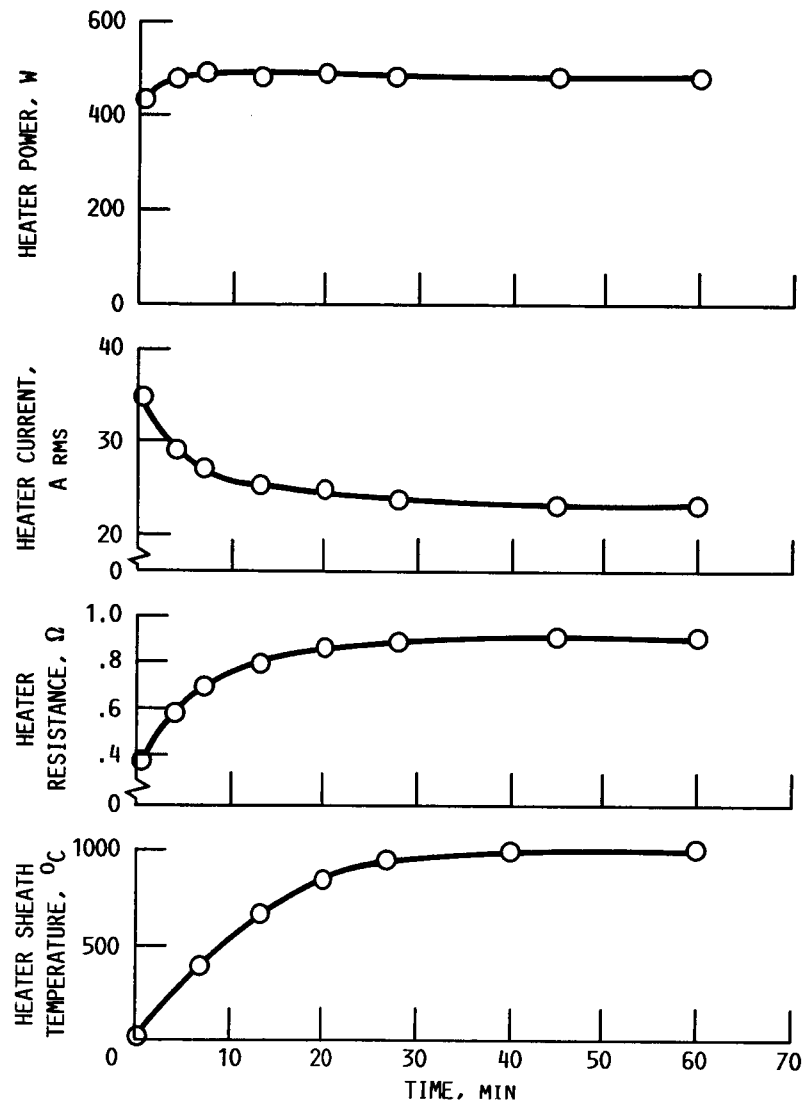FIGURE 7. - RESISTOJET POWER CONTROLLER TEST CONFIGURATION.

FIGURE 8. – HEATER POWER, CURRENT, RESISTANCE, AND
SHEATH TEMPERATURE VERSUS TIME FOR ARGON AT
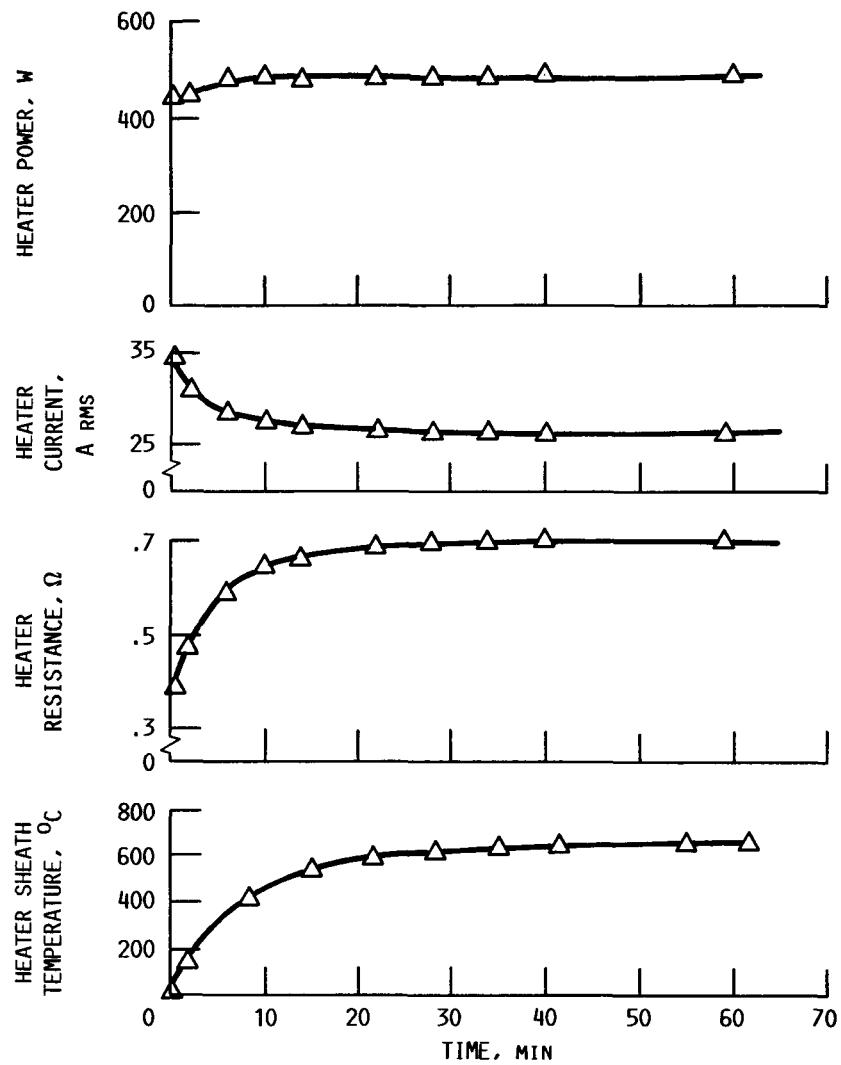30.8 N/CM^2 (44.7 PSIA).

FIGURE 9. - HEATER POWER, CURRENT, RESISTANCE, AND
SHEATH TEMPERATURE VERSUS TIME FOR HELIUM AT
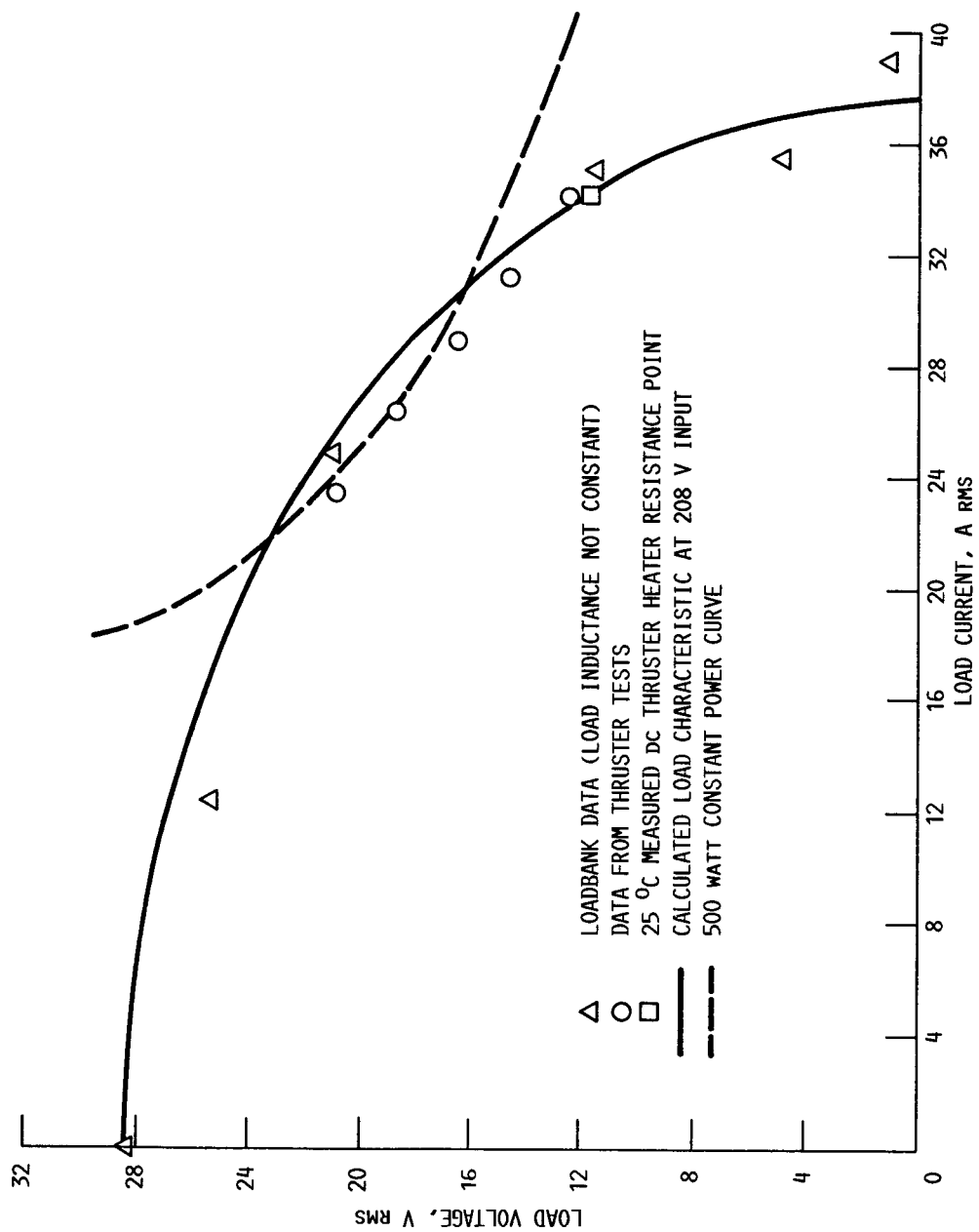29.0 N/CM^2 (42.1 PSIA).

FIGURE 10. - POWER CONTROLLER LOAD CHARACTERISTIC AT THE THRUSTER HEATER.

Legend:
- △ LOADBANK DATA (LOAD INDUCTANCE NOT CONSTANT)
- ○ DATA FROM THRUSTER TESTS
- □ 25 °C MEASURED DC THRUSTER HEATER RESISTANCE POINT
- —— CALCULATED LOAD CHARACTERISTIC AT 208 V INPUT
- –––– 500 WATT CONSTANT POWER CURVE

X-axis: LOAD CURRENT, A RMS
Y-axis: LOAD VOLTAGE, V RMS

1. Report No. NASA TM-89860 AIAA-87-0994	2. Government Accession No.	3. Recipient's Catalog No.
4. Title and Subtitle Resistojet Control and Power for High Frequency ac Buses		5. Report Date
		6. Performing Organization Code 506-42-31
7. Author(s) Robert P. Gruber		8. Performing Organization Report No. E-3527
		10. Work Unit No.
9. Performing Organization Name and Address National Aeronautics and Space Administration Lewis Research Center Cleveland, Ohio 44135		11. Contract or Grant No.
		13. Type of Report and Period Covered Technical Memorandum
12. Sponsoring Agency Name and Address National Aeronautics and Space Administration Washington, D.C. 20546		14. Sponsoring Agency Code

15. Supplementary Notes

Prepared for the 19th International Electric Propulsion Conference cosponsored by the AIAA, DGLR, and JSASS, Colorado Springs, Colorado, May 11-13, 1987.

16. Abstract

Resistojets are operational on many geosynchronous communication satellites which all use dc power buses. Multipropellant resistojets were selected for the Initial Operating Capability (IOC) Space Station which will supply 208 V, 20 kHz power. This paper discusses resistojet heater temperature controllers and passive power regulation methods for ac power systems. A simple passive power regulation method suitable for use with regulated sinusoidal or square wave power was designed and tested using the Space Station multipropellant resistojet. The breadboard delivered 20 kHz power to the resistojet heater. Cold start surge current limiting, a power efficiency of 95 percent, and power regulation of better than 2 percent were demonstrated with a two component, 500 W breadboard power controller having a mass of 0.6 kg.

17. Key Words (Suggested by Author(s)) Resistojet; Control; Power; ac Buses	18. Distribution Statement Unclassified – unlimited STAR Category 33

19. Security Classif. (of this report) Unclassified	20. Security Classif. (of this page) Unclassified	21. No. of pages 32	22. Price* A03